SCIENCE CHINA
Physics, Mechanics & Astronomy

• Research Paper •

May 2010 Vol.53 No.5: 812–817
doi: 10.1007/s11433-010-0074-5

A computational investigation of boron-doped chromium and chromium clusters by density functional theory

GE GuiXian[1*], JING Qun[1] & LUO YouHua[2,3]

[1] *Key Laboratory of Ecophysics and Department of Physics, Normal College, Shihezi University, Xinjiang 832003, China;*
[2] *School of Science, East China University of Science and Technology, Shanghai 200237, China;*
[3] *Institute of Theoretical Physics, School of Physics and Information Optoelectronics, Henan University, Kaifeng 475004, China*

Received June 5, 2009; accepted June 23, 2009; published online April 15, 2010

The geometries, stabilities and electronic properties of Cr_n and Cr_nB (n=2–9) clusters have been systematically investigated by density functional theory. The results suggest that the lowest energy structures for Cr_nB clusters can be obtained by substituting one Cr atom in Cr_{n+1} clusters with B atom. The geometries of Cr_nB clusters are similar to that of Cr_{n+1} clusters except for local structural distortion. The second-order difference and fragmentation energy show Cr_4, Cr_6, Cr_8, Cr_3B, Cr_5B and Cr_8B cluster are the most stable among these studied clusters. The impurity B increases the stabilities of chromium cluster. When B is doped on the Cr_n clusters, cluster geometry does dominate positive role in enhancing their stability. The doped B atom does not change the coupling way of the Cr site in Cr_n clusters, but breaks the symmetry and the Cr atoms are no longer equivalent. The doped B atom increases the total magnetic moments of Cr_n in most cases.

Cr_n and Cr_nB clusters, geometries, electronic properties

PACS: 31.15.A-, 36.40.Cg, 31.15.Ew

Unraveling the structural evolution and physicochemical properties of transition metal clusters are technological important in cluster science. Chromium is unique among transition metals. Its $3d^5 4s^1$ electronic configuration results in strong *d-d* bonding in dimer with short bond length (1.68 Å) [1–4], while bulk chromium is antiferromagnetic with a body-centered-cubic (bcc) structure (nearest Cr–Cr distance: 2.50 Å) [5]. In last decade, the bonding nature and electronic structure in small chromium clusters have been studied by experimental and theoretical methods [6–19]. The geometric and magnetic properties of chromium clusters have been performed by density functional theory (DFT) [20,21]. Bloomfield et al. [22] investigated Cr_8–Cr_{156} and found that magnetic moments range from $0.5\mu_B$ to $1.0\mu_B$ per atom; small chromium clusters possess ferromagnetically coupled spins. Wang et al. [23] studied Cr_nN (n<5) clusters, and found that N is bonded to only three Cr atoms; the coupling of N to the nearest-neighbor Cr is antiferromagnetic. Hence all Cr atoms nearest neighbor to N are coupled ferromagnetically. It is well known that the electronic structure of boron is characterized by three-center bonding. What is the situation for B impurities in chromium clusters? What magnetic moments properties appear? No systematic studies on this subject have been reported to our knowledge. In this paper, we will study this interesting question using density functional theory and provide an *ab initio* structural and electronic investigation for Cr_nB clusters ($n \leqslant 9$). In order to examine the effect of B atom to chromium clusters, geometry optimizations of pure chromium clusters were also calculated using identical method.

1 Computational method

To search the lowest energy structures of Cr_n and Cr_nB

*Corresponding author (email: geguixian@126.com)

clusters, a considerable amount of possible structural isomers have been considered for each size. Full geometry optimizations are performed using density functional theory (DFT) in DMol^3 package [24]. In electronic structure calculations, all electron treatment and double numerical basis including *d*-polarization function (DND) [24] are chosen. The exchange-correlation interaction is treated within the generalized gradient approximation (GGA) using BLYP [25] functional. Self-consistent field calculations are done with a convergence criterion of 10^{-5} hartree on the total energy. The density mixing criterion for charge and spin are 0.2 and 0.5, respectively. The direct inversion in an iterative subspace (DIIS) approach is used to speed up SCF convergence. A 0.005 hartree of smearing is applied to orbital occupation. In the geometry optimization, the converged thresholds are set to 0.004 hartree/Å for the forces, 0.005 hartree for the displacement and 10^{-5} hartree for the energy change. Harmonic vibrational frequencies are computed at the same level to characterize the located structures, and the vibrational frequencies are real for all clusters, confirming that the optimized structure indeed correspond to minima on the potential energy surface. The on-site charges and magnetic moment have been evaluated via Mulliken population analysis [26]. To test the accuracy of theoretical method, CrB and Cr_2 dimer have been calculated. For CrB, the ground state is spin sextet state with the bond length r= 1.958 Å, ω=464.7 cm^{-1}, which is in agreement with previous result (r=2.187 Å, ω=415 cm^{-1} [27]). For Cr_2 dimer, the binding energy (1.23 eV) is in good agreement with corresponding experimental data (E_b=(1.56±0.3) eV [28]). It indicates that the employed BLYP scheme is reliable for CrB and Cr_2 dimer. Thus, one may expect that it can also yield accurate prediction for Cr_n and Cr_nB clusters in this paper.

2 Results and discussion

The lowest energy structures and some metastable isomers of Cr_n and Cr_nB are shown in Figures 1 and 2, respectively. The structures of Cr_n and Cr_nB clusters are denoted by number and letter, where the number denotes the Cr atom number and the letter ranks the isomers in decreasing order of binding energy.

2.1 Growth behavior of different sized chromium clusters

For Cr_3, the triangular and linear structures are considered; the most stable geometry is an equilateral triangular with spin septet state. In addition, a scalene triangular structure

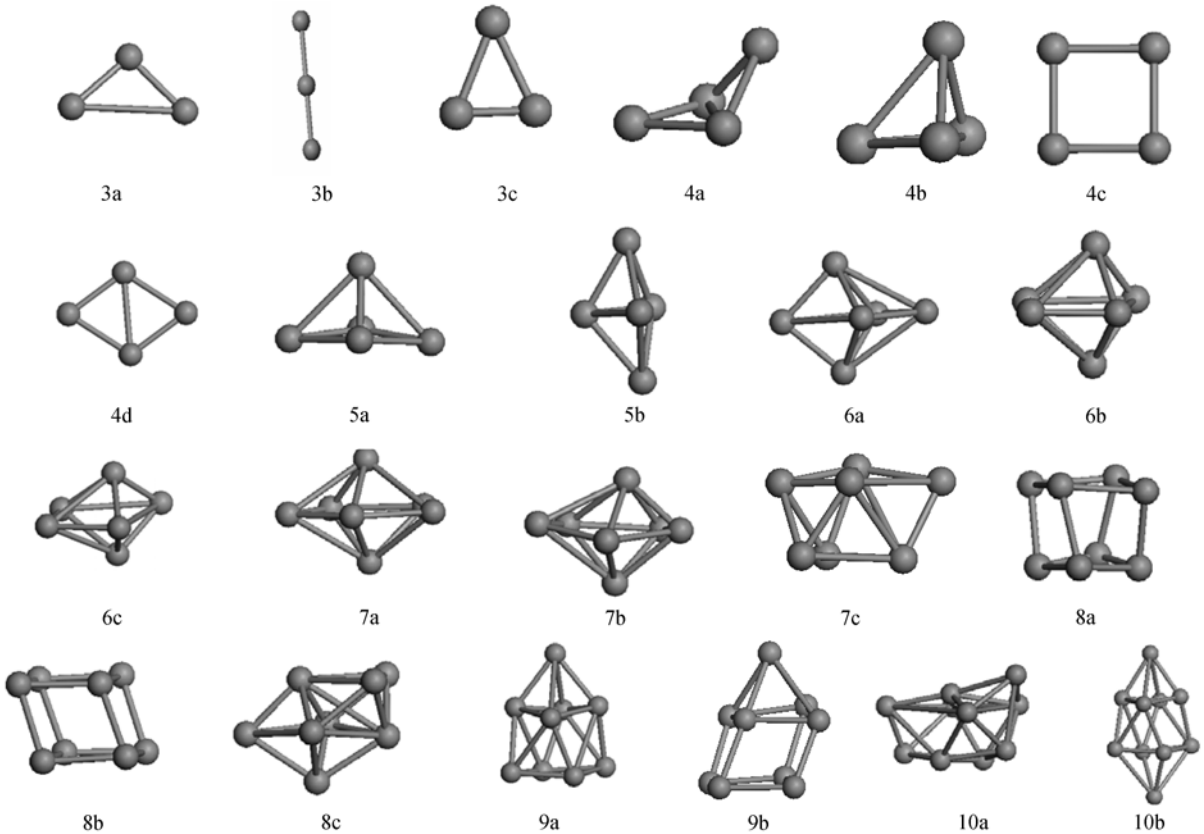

Figure 1 The lowest energy structures for Cr_n (n=2–9) clusters.

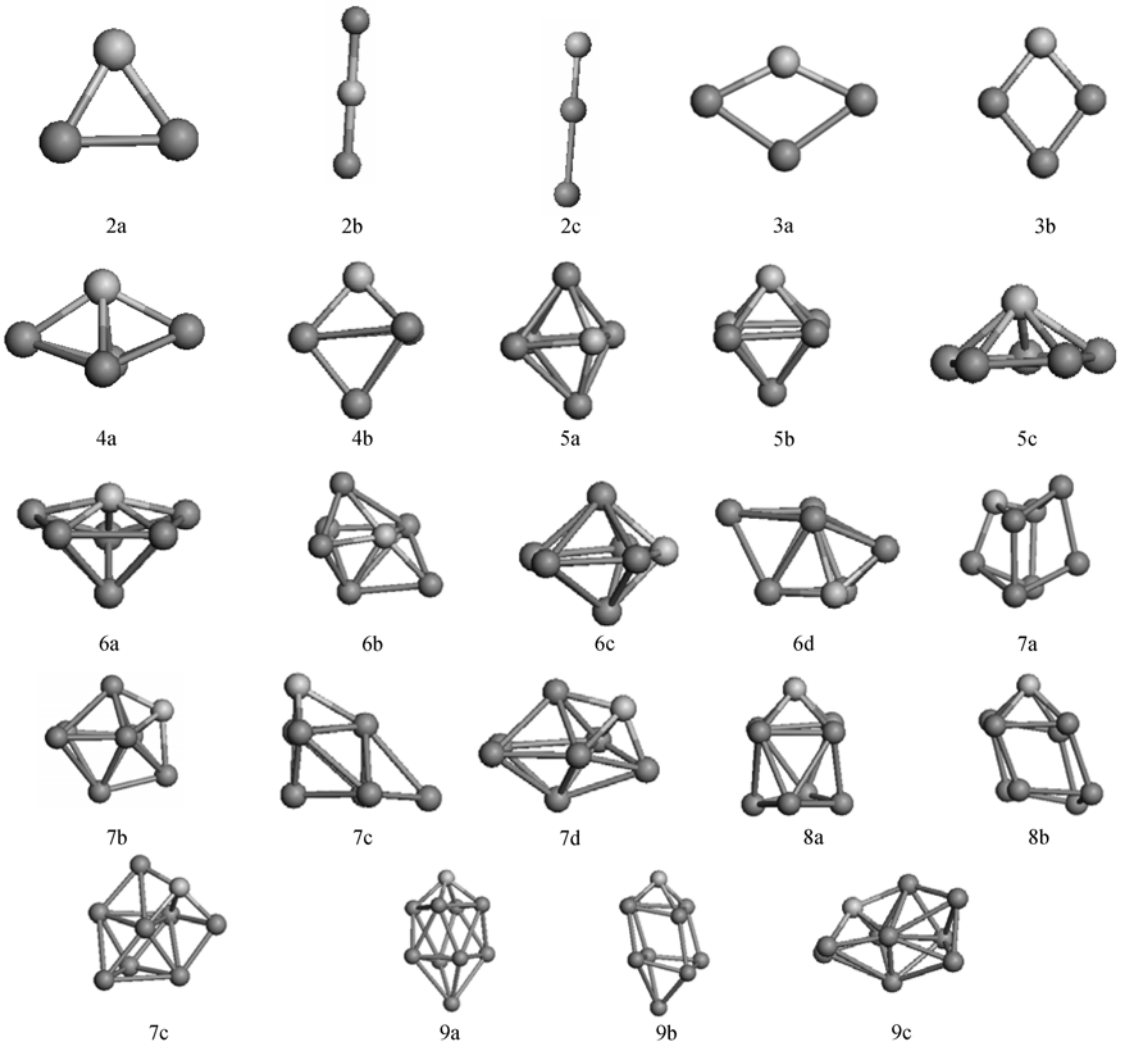

Figure 2 The lowest energy structures of Cr_nB (n=2–9) clusters. The dark circle represents Cr atom and the white circle represents B atom.

with spin septet state is local minimum; its total energy is 0.004999 eV higher than the lowest energy structure. The lowest energy structure of Cr_3 is in agreement with the previously calculated result [18]. The lowest energy structure of Cr_4 is a distorted tetrahedron. As shown in Figure 1, another distorted tetrahedron (C_1) is 2.72 eV higher in energy than the lowest energy structure. Two planar structures, i.e. a planar rectangle (4c) and a rhombus (4d), can be generated by capping one Cr atom on the edge site of the stable Cr_3 frame. For Cr_5 clusters, twin tetrahedron (5a) and trigonal bipyramid (5b) are generated by capping one Cr atom on the Cr_4 cluster (4a). As seen from the total energy, twin tetrahedron (5a) isomer is more stable than trigonal bipyramid isomer (5b). The lowest energy structure of Cr_5 is twin tetrahedron structure (C_s), which is different from the previous result using the local spin density functional approximation (LSD) provided by DMOL package [18].

In analogy to Cr_5 isomer, the edge-capped patterns can also produce the stable structures of Cr_6: the octahedron. The lowest energy structure of Cr_7 is a pentagonal bipyramid (7a) which can be obtained by one Cr atom capping on the edge of Cr_6 cluster (6a). Additionally, the previous local spin density functional approximation (LSD) calculation suggests that the face-capped trigonal prism (C_{2v}) is the lowest energy structure of Cr_7 [18]. However, our calculation does not support the result because this structure is optimized to local minima, and its energy is 2.345 eV higher than the lowest energy structure. Other isomer is a distorted pentagonal bipyramid structure (7b).

For Cr_8 cluster, a distorted quadrangular prism is the lowest energy structure, which is different from Cheng's result [18]. Another face-capped two Cr atoms pentagnoal bipyramid is meta-stable structure. For Cr_9, the lowest energy (9a) and low-lying isomer (9b) are described as one Cr being face capped on the top of 8a and 8b isomer, respectively. According to above analysis, it is found that the geometries of Cr_n can be obtained by capping a Cr atom on the geometry of Cr_{n-1} clusters.

2.2 Growth behavior of different sized boron-doped chromium clusters

For Cr_2B, linear isomers and triangular structure are considered; the most stable structure of Cr_2B (C_{2v}) is the triangular with single spin state which can be obtained by capping B atom on the Cr_2. The lowest energy structure of Cr_3B is a planar quadrangular obtained by B atom substituting a Cr atom in Cr_4 (4c). For Cr_4B cluster, the most stable structure is obtained by B substituting the apical Cr atom in the Cr_5 isomer (5a). The 4b isomer is yielded with the top Cr atom being substituted by B in the Cr_5 cluster (5b).

The lowest energy structure of Cr_5B is obtained by edge-substituting the Cr with a B in the Cr_6 cluster (6a). The isomer obtained by top-substituting the Cr with a B in the Cr_6 cluster is 0.77578 eV higher in energy than the lowest energy structure. Therefore, the different substituted positions of B atom in the Cr_{n+1} lead to different Cr_nB isomers. The other isomer is a pentagonal pyramid, and its energy is 0.94094 eV higher than the lowest energy structure. The lowest energy structure of Cr_6B is obtained by face-capped two Cr atoms on the 4(a).

The lowest energy structure of Cr_7B can be obtained by substituting a Cr atom by B on the lowest energy structure of Cr_8. The bicapped rhombic bipyramid isomer (7b) is obtained when one Cr atom in the Cr_8 (8c) isomer is substituted by B. Another structure of Cr_7B cluster (7c) is 0.19647 eV higher in energy than the lowest energy structure. Cr_7B (7d) obtained by capping one B atom on the lowest energy structure of Cr_7 cluster is 0.2087 eV less stable than the lowest energy structure. The lowest energy structure of Cr_8B is obtained by substituting a Cr atom with a B atom in the lowest energy of Cr_9 cluster. For Cr_9B clusters, the lowest energy structure is bipyramid quadrangular anti-prism with one top Cr atom in Cr_{10} (10b) being substituted by B. The other two isomers are 0.0022739 and 0.17986 eV higher than the lowest energy structure, respectively.

From analysis, it is found that one B atom does not change the geometrical configurations of host clusters; But the energy ordering of some isomers with small energy difference probably reverses.

2.3 Relative stability and electronic properties

It is well known that the relative stability of different sized clusters can be predicted by calculating the averaged binding energy. The averaged binding energies for Cr_n and Cr_nB clusters can be defined as

$$E_b = [nE_T(\mathrm{Cr}) - E_T(\mathrm{Cr})_n]/n, \quad (1)$$

$$E_b' = [nE_T(\mathrm{Cr}) + E_T(\mathrm{B}) - E_T(\mathrm{Cr}_n\mathrm{B})]/(n+1), \quad (2)$$

where E_T (Cr_n), E_T (Cr_nB), E_T (Cr) and E_T (B) represent the total energies of the most stable Cr_n, Cr_nB, Cr and B, respectively.

The calculated results on the averaged binding energies for Cr_n and Cr_nB are plotted in Figure 3. As shown in Figure 3, the averaged binding energy increases dramatically as Cr_n size increases. It reflects that the stabilities of Cr_n have been enhanced with clusters size increasing. The averaged binding energies of Cr_nB are larger than that of Cr_n. It reveals that the doped B atom enhances the stability of Cr_n clusters.

The fragmentation energy (E_F) is another useful quantity for determining the stability of clusters. The fragmentation energy of the total energies for Cr_n and Cr_nB clusters are presented in Figure 4. The fragmentation energy can be defined by

$$E_F(n) = E_T(\mathrm{Cr}) + E_T(\mathrm{Cr}_{n-1}) - E_T(\mathrm{Cr}_n), \quad (3)$$

$$E_F'(n) = E_T(\mathrm{Cr}_{n-1}\mathrm{B}) + E_T(\mathrm{Cr}) - E_T(\mathrm{Cr}_n\mathrm{B}), \quad (4)$$

where E_T (Cr), E_T (Cr_{n-1}), E_T ($Cr_{n-1}B$), E_T (B), E_T (Cr_nB), and E_T (Cr_n) represent the total energies of the most stable Cr, Cr_{n-1}, $Cr_{n-1}B$, B, Cr_nB and Cr_n, respectively. As shown in Figure 4, the local peaks of E_F (n) appear at the sizes of 4, 6 and 8, indicating these clusters are more stable than their neighboring size. For Cr_nB, the local maxima of E'_F (n) appear at the sizes of 3, 5 and 8, showing these clusters are more stable than their neighboring size.

The relative stabilities of these clusters can be better understood by calculating the second order difference of cluster energies $\Delta_2E(n)$ is defined as

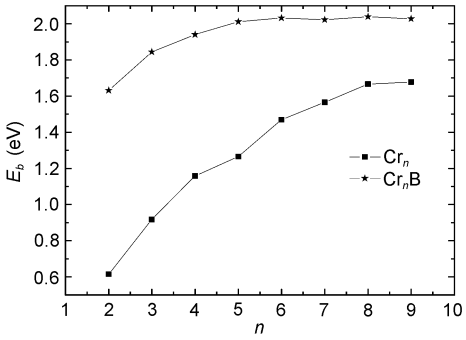

Figure 3 Binding energy versus cluster size for Cr_n and Cr_nB clusters.

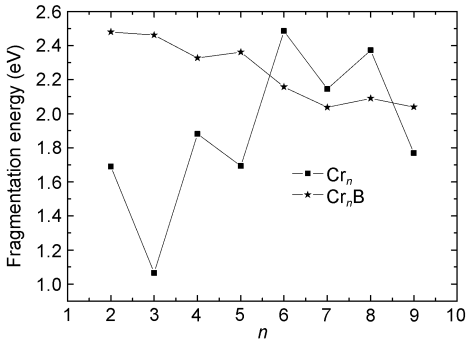

Figure 4 The fragmentation energy of the total energies for Cr_n and Cr_nB clusters.

$$\Delta_2 E(n) = E(n+1) + E(n-1) - 2E(n), \quad (5)$$

where $E(n)$ is the total energy of clusters. The second order difference for Cr_n and Cr_nB clusters are presented in Figure 5. The second order differences of Cr_n appear odd-even alternation. The values with even number Cr atom are larger than that of neighboring odd number Cr atom, indicating Cr_4, Cr_6 and Cr_8 clusters are the most stable geometry which is consistent with the result of fragmentation energies. For Cr_nB clusters, particularly high peaks are found at n=3, 5, 8, indicating that these clusters are more stable than its neighboring clusters, which is also consistent with the result of fragmentation energies shown in Figure 4. For Cr_3B and Cr_5B clusters, geometry does dominate positive role in enhancing their stability; otherwise, an inverse odd-even alternation pattern should occur. According to above analysis, it is found that B impurity can change the magic behavior for some host clusters.

The energy gaps between the highest occupied molecular orbital (HOMO) and the lowest unoccupied molecular orbital (LUMO) are plotted in Figure 6. The gaps of Cr_n appear odd-even alternation, and the gaps with even number Cr are larger than that of neighboring odd number Cr. Namely, the gap for the Cr_n clusters with even electronic numbers are larger than those with odd electronic numbers.

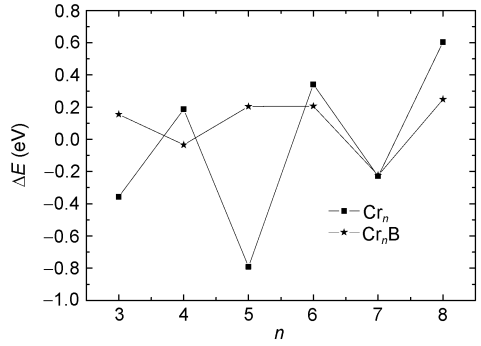

Figure 5 Second finite difference of the total energies for Cr_n and Cr_nB clusters.

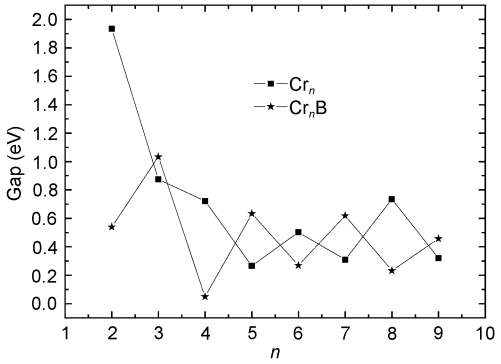

Figure 6 The HOMO-LUMO Gaps of the total energies for Cr_n and Cr_nB clusters.

The valence electronic configuration of Cr is $3d^5s^1$. There are full sharing electrons for the clusters with even number Cr which corresponds to the close-shell structure, and their chemical activities are comparatively weaker than those of the clusters with odd number electrons. So such odd-even alternation is governed by electron-pairing effect. The HOMO-LUMO gaps of Cr_nB also appear odd-even alternation, but the gap of even number cluster are smaller than that of neighboring odd number cluster, which indicates cluster geometry does dominate positive role in enhancing their stability for Cr_nB.

2.4 Magnetic properties

We now discuss the effect of B doping on the magnetic properties of Cr_n clusters. In Table 1, we list the total magnetic moment of Cr_nB and Cr_n. The total magnetic moments of Cr_n (n=2–9) are $0.000\mu_B$, $6.001\mu_B$, $0.000\mu_B$, $3.999\mu_B$, $0.000\mu_B$, $6.000\mu_B$, $0.001\mu_B$, $3.999\mu_B$, respectively. The total magnetic moments with even number Cr are quenched, and the total magnetic moments with odd number Cr appear 4 and 6 alternating phenomenon; maybe there is other important information. Further and larger size cluster investigation will be done in our future research.

The Cr_2 is antiferromagnetic with a total magnetic moment of $0\mu_B$. The coupling between the magnetic moments at the Cr site in Cr_2B is also antiferromagnetic, which is different from the coupling between the magnetic moments at the Cr site in Cr_nN clusters [23]. In Cr_2B, the presence of B breaks the symmetry and the Cr atoms are no longer equivalent; the magnetic moment at each of the Cr site is 3.921, $-4.059\mu_B$, respectively, and B atom carries a small magnetic moment, namely, $-0.097\mu_B$. The total magnetic moment of Cr_2B is $0.235\mu_B$: an enhancement over that in Cr_2. The doped B atom does not change the coupling way of the Cr site for Cr_2B, which is different from the impact of N on Cr in Cr_nN clusters [23]. For Cr_3B cluster, the total magnetic moment is $3.995\mu_B$, and the alignments between the magnetic moments at the Cr site appear ferromagnetically or antiferromagnetically. The doped B atom does not change the coupling way of the Cr site in Cr_3, and similar phenomenon is found for other size cluster. The total magnetic moment of Cr_3B is reduced than that of Cr_3 cluster.

Table 1 The total magnetic moments (M/μ_B) of Cr_n and Cr_nB ($n\geqslant 9$)

n	Cr_n	Cr_nB
	M	M
2	0.000	0.235
3	6.001	3.995
4	0.000	0.951
5	3.999	4.779
6	0.000	0.787
7	6.000	3.000
8	0.001	0.150
9	3.999	4.892

The local magnetic moments of the Cr sites also appear ferromagnetic or antiferromagnetic aligment for $n \geqslant 4$. In Cr_nB clusters (n=4, 5, 6, 8, 9), the total magnetic moments are enhanced compared to that of corresponding Cr_n clusters, respectively. For Cr_7B clusters, the total magnetic moment is reduced compared to Cr_7 cluster. The doped B atom increases the total magnetic moments of Cr_n in most cases. Our result may have some guidance significance for increasing the magnetic moments of Cr_n.

3 Conclusions

In summary, we have studied the structure and electronic properties of Cr_n and Cr_nB (n=2–9) clusters including their equilibrium structures, binding energy, HOMO-LUMO gaps, magnetic properties and relative stabilities. The result indicates the lowest energy structures of Cr_nB (n=2–9) clusters can be obtained by substituting one Cr atom of their corresponding chromium clusters with a B atom. The Cr_nB clusters have similar geometrical configurations to those of Cr_{n+1} clusters except for local structural distortion. The calculated second-order difference and fragmentation energy show that Cr_4, Cr_6, Cr_8, Cr_3B, Cr_5B and Cr_8B cluster are the most stable among those studied clusters. It is concluded that impurity B increases the stabilities of chromium cluster by analyzing electronic properties. When B is doped on the Cr_n clusters, cluster geometry does dominate positive role in enhancing their stability. The doped B atom does not change the coupling way of the Cr site in Cr_n clusters, but breaks the symmetry and the Cr atoms are no longer equivalent. The doped B atom increases the total magnetic moments of Cr_n in most cases.

This work was supported by the Foundation Start Up for High Level Talents of Shihezi University, China (Grant No. RCZX200747).

1 Kundig E P, Moskovits M, Ozin G. Matrix synthesis and characterization of dichromium, Cr_2. Nature, 1975, 254: 503–504
2 Andersson K. The electronic spectrum of Cr_2. Chem Phys Lett, 1995, 237: 212–221
3 Casey S M, Leopold D G. Negative ion photoelectron spectroscopy of Cr_2. J Phys Chem, 1993, 97: 816–830
4 Goodgame M M, Goddard W A. Modified generalized valence-bond method: A simple correction for the electron correlation missing in generalized valence-bond wave functions; prediction of double-well states for Cr_2 and Mo_2. Phys Rev Lett, 1985, 54: 661–664
5 Kittel C. Introduction to Solid State Physics. 6th ed. New York: John Wiley and Sons, Inc, 1986
6 Anderson A B. Structures, binding energies, and charge distributions for two to six atom Ti, Cr, Fe, and Ni clusters and their relationship to nucleation and cluster catalysis. J Chem Phys, 1976, 64: 4046–4055
7 Bauschlicher C W, Partridge Jr H. Cr_2 revisited. Chem Phys Lett, 1994, 231: 277–282
8 Desmarais N, Reuse F A, Khanna S N. Magnetic coupling in neutral and charged Cr_2, Mn_2, and CrMn dimers. J Chem Phys, 2000, 112: 5576–5584
9 Andersson K, Roos B O, Malmqvist P Å, et al. The Cr_2 potential energy curve studied with multiconfigurational second-order perturbation theory. Chem Phys Lett, 1994, 230: 391–397
10 Andersson K. The electronic spectrum of Cr_2. Chem Phys Lett, 1995, 237: 212–221
11 Weber S E, Reddy B V, Rao B K, et al. Chemically induced changes in the magnetic moments in transition metal monomers and dimers. Chem Phys Lett, 1998, 295: 175–180
12 DiLella D P, Limm W, Lipson R H, et al. Dichromium and trichromium. J Chem Phys, 1982, 77: 5263–5266
13 Pellin M J, Gruen D M. Emission, ground, and excited state absorption spectroscopy of Cr_2 isolated in Ar and Kr matrices. J Chem Phys, 1983, 79: 5887–5893
14 Michalopoulos D L, Geusic M E, Hansen S G, et al. The bond length of Cr_2. J Phys Chem, 1982, 86: 3914–3916
15 Bondybey V E, English J H. Electronic structure and vibrational frequency of Cr_2. Chem Phys Lett, 1983, 395: 443–447
16 Riley S J, Parks E K, Pobo L G, et al. The $A \leftarrow X$ transition in Cr_2: Predissociation, isotope effects, and the 1–1 sequence band. J Chem Phys, 1983, 79: 2577–2582
17 Casey S M, Leopold D G. Negative ion photoelectron spectroscopy of Cr_2. J Phys Chem, 1993, 97: 816–830
18 Cheng H, Wang L S. Dimer growth, structural transition, and antiferromagnetic ordering of small chromium clusters. Phys Rev Lett, 1996, 77: 51–54
19 Wang L S, Wu H, Cheng H. Photoelectron spectroscopy of small chromium clusters: Observation of even-odd alternations and theoretical interpretation. Phys Rev B, 1997, 55: 12884–12887
20 Kohl C, Bertsch G. Noncollinear magnetic ordering in small chromium clusters. Phys Rev B, 1999, 60: 4205–4211
21 Reddy B V, Khanna S N, Jena P. Structure and magnetic ordering in Cr_8 and Cr_{13} clusters. Phys Rev B, 1999, 60: 15597–15600
22 Bloomfield L A, Deng J, Zhang H, et al. Magnetism and magnetic isomers in chromium clusters. Proceedings of the International Symposium on Cluster and Nanostructure Interfaces. Singapore: World Scientific, 2000
23 Wang Q, Sun Q, Rao B K, et al. Nitrogen-induced magnetic transition in small chromium clusters. J Chem Phys, 2003, 119: 7124–7130
24 Delley B. An all-electron numerical method for solving the local density functional for polyatomic molecules. J Chem Phys, 1990, 92: 508–517
25 Lee C, Yang W, Parr R G. Development of the Colle-Salvetti correlation-energy formula into a functional of the electron density. Phys Rev B, 1988, 37: 785–789
26 Mulliken R S. Electronic population analysis on LCAO-MO molecular wave functions. II. Overlap populations, bond orders, and covalent bond energies. J Chem Phys, 1955, 23: 1841–1846
27 Wu Z J. Density functional study of 3d-metal monoborides. J Mol Struc-Theochem, 2005, 728: 167–172
28 Kant A, Straws B. Dissociation energy of Cr_2. J Chem Phys, 1966, 45: 3161–3162